Inorganica Chimica Acta, 112 (1986) 113–117

The Preparation, Crystal Structure and Thermal Analysis of bis(ferrocenium)[μ_2-oxo bis(trichloroferrate(III))]

P. CARTY*

School of Applied Consumer Sciences, Newcastle-upon-Tyne Polytechnic, Newcastle-upon-Tyne NE1 8ST, U.K.

K. C. CLARE, J. R. CREIGHTON, E. METCALFE, E. S. RAPER

School of Chemical and Life Sciences, Newcastle-upon-Tyne Polytechnic, Newcastle-upon-Tyne NE1 8ST, U.K.

and H. M. DAWES

Department of Chemistry, Queen Mary College, University of London, Mile End Road, London, U.K.

Received May 22, 1985

Abstract

Ferrocene reacts with iron(III) chloride in the presence of water producing bis(ferrocenium)[μ_2-oxo bis(trichloroferrate(III))], $[Fe(\mu^5\text{-}C_5H_5)_2][Fe_2OCl_6]$. Electronic and vibrational spectra have established the presence of ferrocenium cations in the compound. Room temperature magnetic measurements are consistent with antiferromagnetic coupling between the iron(III) atoms, with the magnetic exchange occurring through the bridging oxygen atom. Crystal structure analysis has shown the anion to consist of two $FeOCl_3$ tetrahedra bridged by means of the shared oxygen atom. Within the anion there is an average Fe–Cl distance of 2.197 Å, an Fe–O distance of 1.749 Å and an Fe–O–Fe angle of 162.1°. Thermal analysis indicates a three-stage degradation mechanism for the complex in air.

Introduction

One of the simplest and most characteristic reactions of ferrocene is its oxidation to the cation through loss of one electron from the iron atom. Oxidation may be brought about electrolytically [1], photolytically [2] or by a wide variety of organic and inorganic compounds [3]. Substituted ferrocenium ions can be stabilised with large anions such as BF_4^-, ClO_4^-, PF_6^- etc. [4]. Removal of an electron from the e_2'' orbital in ferrocene to produce the ferrocenium ion substantially lengthens the (cp–cp) distance [5]. This weakening of the (M–cp) bonds in ferrocenium is reflected in the lower stability of ferrocenium compounds compared with ferrocene [6].

The interest in this compound is two-fold. Ferrocene is used as a smoke suppressant in polymers (e.g. PVC) but the volatility of ferrocene can lead to its gradual loss from the polymer. Ferrocenium salts are also active as smoke suppressants [7] and should be less volatile. Binuclear μ-oxo bridged di-iron(III) complexes are of interest as model compounds for the biologically important non-heme oxygen transport proteins myohemerythrin and hemerythrin and also the enzyme ribonucleotide reductase [8].

Experimental

Starting Materials

Ferrocene and anhydrous iron(III) chloride were obtained from BDH.

Preparation

Ferrocene was twice recrystallised from ethanol. Anhydrous iron(III) chloride was used directly without further purification and was handled in a nitrogen filled glove bag. Diethyl ether and tetrahydrofuran (THF) were thoroughly dried over sodium wire and used without further purification. Preparation of the ferrocenium compound was carried out as described in reference [4].

Dropwise addition of a solution of ferrocene in dry diethyl ether under nitrogen to a stirred solution of anhydrous iron(III) chloride in the same solvent afforded an instantaneous blue precipitate in almost quantitative yield. Careful recrystallisation of this product from dry THF gave deep blue orthorhombic air-stable crystals of $[(C_5H_5)_2Fe]_2[Fe_2OCl_6]$. *Anal.* Found: C, 33.87; H, 2.72; Cl, 29.32. Calc.: C, 33.71; H, 2.83; Cl = 29.86%. The presence of oxygen in the complex was derived from water in the iron(III) chloride which, although nominally anhydrous, was found by thermal analysis to contain sufficient water to provide the bridging oxygen atoms in the product anion.

*Author to whom correspondence should be addressed.

0020-1693/86/$3.50

Physical Measurements

Infrared spectra were obtained as CsI discs in the range 4000–200 cm^{-1} on a Perkin Elmer 684 spectrophotometer. Raman spectra were obtained in the range 1000–200 cm^{-1} using a 488 nm Ar laser line with the sample in the form of a spinning disc to minimise decomposition. The Raman spectra obtained were of rather poor quality owing to a high fluorescence background.

Magnetic measurements were performed on powdered samples using a Gouy balance at room temperature.

Thermal analysis curves (TG, DTG and DTA) were obtained using Stanton-Redcroft TG 750 and DTA 673/4 instruments. Crystalline and powdered sample masses in the range (1.6–2.0 mg) were used to record the thermal analysis curves. Heating rates were in the range 5 to 50 °C min^{-1}. Platinum crucibles were used for the TG data and 3 cm quartz crucibles for the DTA results. Gas flow rates were 10 cm^3 min^{-1} (air) for the TG and 100 cm^3 min^{-1} (nitrogen) for the DTA determinations. Calibration details for the quantitative DTA are reported elsewhere [9]. X-ray powder photographs were recorded with a Philips XDC-700 camera incorporating Guinier–Hagg parafocussing geometry and monochromatised Cu Kα (λ = 1.5405 Å) radiation.

Crystal Structure Analysis

Intensity data were collected on a Nonius CAD-4 diffractometer using Mo Kα radiation and an ω-2θ scan mode as previously described [10]. A summary of crystallographic data is given in Table I.

TABLE I. Crystallographic Data.

Compound	$[cp_2Fe]_2[Fe_2OCl_6]$
M_r	712.49
Crystal system	Orthorhombic
a (Å)	14.564(3)
b (Å)	13.372(3)
c (Å)	14.213(4)
U (Å^3)	2767.989
Space group	*Pnma*
Z	4
D_c (g cm^{-3})	1.71
D_m (g cm^{-3})	–
$F(000)$	1416
μ(Mo Kα) (cm^{-1})	25.29
2θ range (deg)	3–60
Total unique data	4188
Observed data	1952
Significance test	$F_o^2 > 4\sigma(F_o)^2$
Number of parameters	151
Weighting scheme coefficient in $w = 1[\sigma^2(F_o) + gF_o^2]$	0.0006
Final $R = \Sigma\Delta F/\Sigma 1F_o 1$	0.0606
$R' = (\Sigma w\Delta F^2/\Sigma wF_o^2)^{1/2}$	0.0695

Solution by the heavy atom method was initially attempted in the non-centrosymmetric space group $Pna2_1$ after the positions of four iron atoms were obtained by Patterson-search techniques [11]. Isotropic refinement revealed high correlation between atomic coordinates with the x and y coordinates for two iron atoms approaching the same value so a transformation was made to the centrosymmetric space group *Pnma*. Two iron atoms were located at $y = 0.25$ with a carbon atom from both of the two cyclopentadienyl rings in each ferrocenium ion also located on the mirror plane. A further iron atom was discovered in a general position linked through a bridging oxygen atom at $y = 0.25$ to another trichloroferrate(III) unit. Refinement proceeded by full-matrix, least squares [12] incorporating anisotropic thermal parameters for all non-hydrogen atoms. Empirical absorption corrections were applied together with a correction using the DIFABS method [13]. Several carbon–carbon distances within the cyclopentadienyl rings were D-fixed [12] at 1.42 Å. Hydrogen atoms could not be located.

Final fractional coordinates are listed in Table II, bond distances and angles in Table III. Anisotropic temperature factors and structure factor Tables have been deposited with the Editor-in-Chief.

TABLE II. Atomic Coordinates (×10^4) with e.s.d.s in Parentheses.

Atom	x	y	z
Fe(1)	3565(1)	2500	1374(1)
Fe(2)	5172(1)	2500	7047(1)
Fe(3)	2379(1)	1208(1)	4542(1)
Cl(1)	1992(2)	408(2)	3258(2)
Cl(2)	1435(2)	760(2)	5676(2)
Cl(3)	3788(2)	749(2)	4899(2)
O	2314(6)	2500	4363(6)
C(1)	2866(6)	1965(6)	207(6)
C(2)	2422(5)	1645(6)	1053(6)
C(3)	2143(7)	2500	1582(9)
C(1A)	4887(7)	1986(14)	1333(9)
C(2A)	4455(9)	1621(11)	2177(9)
C(3A)	4237(12)	2500	2680(11)
C(4)	6484(6)	3020(8)	6892(7)
C(5)	5949(7)	3317(7)	6114(8)
C(6)	5611(11)	2500	5640(10)
C(4A)	3879(6)	1899(10)	7237(8)
C(5A)	4422(8)	1671(8)	8033(8)
C(6A)	4775(12)	2500	8499(12)

Results and Discussion

Magnetic Properties

A magnetic moment ($\mu_B = 6.73$) at 293 K was determined. This is rather low but reflects the firmly

TABLE III. Bond Lengths and Angles with e.s.d.s in Parentheses.

Bond lengths (Å)			
Cl(1)–Fe(3)	2.190(4)	Cl(2)–Fe(3)	2.201(5)
Cl(3)–Fe(3)	2.201(4)	O–Fe(3)	1.749(4)
Fe(3)–Fe(3)[a]	3.455(5)	C(1)–Fe(1)	2.074(10)
C(2)–Fe(1)	2.070(10)	C(3)–Fe(1)	2.092(13)
Cp(1)–Fe(1)	1.684	C(1A)–Fe(1)	2.045(12)
C(2A)–Fe(1)	2.089(13)	C(3A)–Fe(1)	2.099(16)
Cp(2)–Fe(1)	1.691	C(4)–Fe(2)	2.045(10)
C(5)–Fe(2)	2.057(11)	C(6)–Fe(2)	2.099(16)
Cp(3)–Fe(2)	1.686	C(4A)–Fe(2)	2.066(11)
C(5A)–Fe(2)	2.095(11)	C(6A)–Fe(2)	2.143(18)
Cp(4)–Fe(2)	1.693	C(2)–C(1)	1.431(12)
C(1)–C(1)[a]	1.432(17)	C(3)–C(2)	1.427(11)
C(2A)–C(1A)	1.438(19)	C(1A)–C(1A)[a]	1.375(38)
C(3A)–C(2A)	1.412(15)	C(5)–C(4)	1.410(9)
C(4)–C(4)[a]	1.389(22)	C(6)–C(5)	1.375(9)
C(5A)–C(4A)	1.413(10)	C(4A)–C(4A)[a]	1.608(28)
C(6A)–C(5A)	1.390(10)		
Bond angles (deg)			
Cl(2)–Fe(3)–Cl(1)	108.4(2)	Cl(3)–Fe(3)–Cl(1)	107.2(2)
Cl(3)–Fe(3)–Cl(2)	109.7(2)	O–Fe(3)–Cl(1)	110.4(4)
O–Fe(3)–Cl(2)	110.0(4)	O–Fe(3)–Cl(3)	111.0(4)
Fe(3)–O–Fe(3)[a]	162.1(5)	Cp(1)–Fe(1)–Cp(2)	180.0
Cp(3)–Fe(2)–Cp(4)	178.1	C(3)–C(2)–C(1)	109.4(8)
C(2)–C(1)–C(1)	107.4	C(2)–C(3)–C(2)[a]	106.4
C(3A)–C(2A)–C(1A)	103.8(16)	C(2A)–C(1A)–C(1A)[a]	109.8
C(2A)–C(3A)–C(2A)[a]	112.6	C(6)–C(5)–C(4)	111.0(11)
C(5)–C(4)–C(4)[a]	106.4	C(5)–C(6)–C(6)[a]	105.3
C(6A)–C(5A)–C(4A)	114.6(13)	C(5A)–C(4A)–C(4A)[a]	102.5
C(5A)–C(6A)–C(6A)[a]	105.8		

Symmetry code: *x, y, z*; except [a] *x*, 0.5 *y*, *z*.

established tendency of μ_2-oxo di-iron(III) complexes to exhibit antiferromagnetism via a super exchange pathway between two high spin Fe(III) atoms across the oxygen bridge [14, 15].

Assuming μ_B values of 2.2–2.3 for the ferrocenium cation [16], the magnetic moment (μ_B) per Fe atom in the anion is in the region of 1.1–1.2 which is lower than the values (μ_B *ca.* 1.9) typically obtained for μ_2-oxo di-iron(III) complexes at 293 K.

Vibrational Spectra

Features attributable to both the ferrocenium cation and the oxygen bridged anion were observed in the infra-red spectrum. The cyclopentadienyl ring vibrations were in most cases higher than for ferrocene by up to 10 cm^{-1}, reflecting the weaker metal–ligand bonding typical of ferrocenium ions [4].

An intense band found at 851 cm^{-1}, with a shoulder at 868 cm^{-1} is characteristic of $\mu_2$oxo di-iron(III) complexes and is assigned to ν_{as}(Fe–O–Fe). This is typical of this moiety, but a little lower than the asymmetric stretching frequency observed at 870 cm^{-1} for the compound $[C_5H_6N]_2[Cl_3FeOFeCl_3]$, C_5H_5N reported by Solbrig *et al.* [17].

Wide variations in the value of ν_{as} (Fe–O–Fe) have been recently reported; much lower values (751 and 730 cm^{-1}) are known for compounds with low Fe–O–Fe bond angles (124.6° and 118.3°) respectively [8, 18]. A corresponding Raman band at 852 cm^{-1} is observed.

Although Solbrig *et al.* [17] assigned a Raman band at 458 cm^{-1} to ν_s(Fe–O–Fe), the presence of ferrocene bands in this region of the spectrum together with poor quality Raman spectra does not permit assignment of ν_s(Fe–O–Fe) in this study. Two iron–chlorine frequencies were detected; ν_{as}(Fe–Cl) at 360 cm^{-1} and ν_s(Fe–Cl) at 318 cm^{-1} in the infra-red which is also observed as a shoulder at 320 cm^{-1} in the Raman spectrum. This is in good agreement with the reported values of 360 cm^{-1} (IR) and 357 cm^{-1} (Raman) for ν_{as}(Fe–Cl) and 311 cm^{-1} for ν_s(Fe–Cl) [17].

Electronic Spectrum

The UV-Vis absorption spectrum exhibited characteristic ferrocenium bands in acetonitrile at 617 nm ($\epsilon_{max} \sim 450$) and 248 nm ($\epsilon_{max} \sim 24\,000$) overlapping with bands attributable to the anion at 217 nm

($\epsilon_{max} \sim 13\,000$), 287 nm ($\epsilon_{max} \sim 19\,000$) and a shoulder at 316 nm ($\epsilon_{max} \sim 12\,000$). However, the solutions were unstable and these peaks were gradually replaced over several minutes by peaks appearing at 246 nm and 357 nm, probably reflecting the formation of tetrachloroferrate(III) [24].

Crystal Structure

The structure contains two unrelated ferrocenium cations, each of which is sited on a mirror plane which contains the iron atom and one carbon from each ring. The two cations differ however in that one (containing Fe(1)) has an exactly eclipsed cp/cp configuration whilst the other (Fe(2)) has a staggered configuration (Fig. 1).

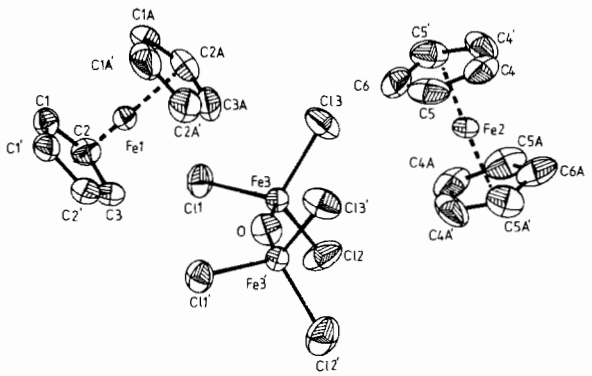

Fig. 1. Labelled perspective diagram of $[(C_5H_5)_2Fe]_2$-$[Fe_2OCl_6]$.

Perpendicular ring cp–cp distances (3.375 and 3.379 Å); average Fe–cp distance (1.688 and 1.690 Å) and average Fe–C distances (2.075 and 2.084 Å) are similar to those reported for other ferrocenium salts [5, 19].

Oxo-bridged di-iron(III) centres are ubiquitous species of considerable biochemical importance [8], they also frequently result from the hydrolytic polymerisation of Fe(III) species [20]; complexes containing such species have been reviewed [14].

The structure of the anion is very similar to that reported for pyridinium[μ_2-oxo-bis trichloroferrate-(III)]–pyridine [15]. In both cases two $FeOCl_3$ tetrahedra are bridged by means of the shared oxygen atom; the anions also possess crystallographically imposed C_s symmetry.

The Fe–Cl bond lengths (2.190–2.201 Å) are similar to those reported for tetrahedral $FeCl_4^-$ anions (2.182–2.187(1) Å [21] and 2.180–2.186(2) Å [22]). The angles O–Fe–Cl and Cl–Fe–Cl are close to the tetrahedral value with the mean value of the former rather larger and that of the latter rather smaller than the ideal value as was found in the pyridinium complex [15].

The Fe–O distance (1.749 Å) together with that of the pyridinium complex, (1.755(3) Å), are the shortest yet reported for μ_2-oxo-diiron(III) complexes [14]. The angle Fe–O–Fe (162.1°) falls in the upper portion of the range of such angles (139–178°) reported for the above mentioned complexes.

Thermal Analysis

The complex degrades in air, over the temperature range 0–1000 °C to iron(III) oxide, this end product being identified by X-ray powder diffraction. Actual (60.0%) and theoretical (55.1%) mass losses differ by an amount which exceeds the normal experimental

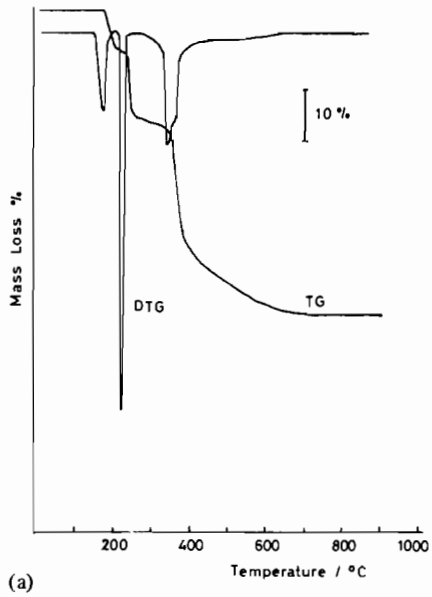

(a)

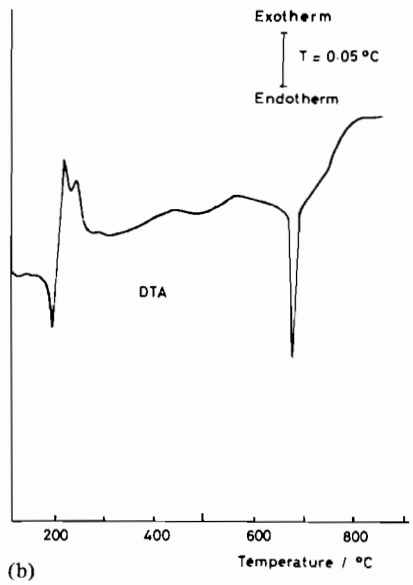

(b)

Fig. 2. Thermal analysis curves: (a) TG/DTG, heating rate 50 °C min^{-1} in flowing air. (b) DTA, heating rate 20 °C min^{-1} in flowing nitrogen.

error (±2.0%) of the instrument. Such differences are common among compounds which are prone to sublimation.

The TG and DTG curves each consist of three stages, the last of which is complex in character (see Fig. 2). The initial mass loss (8.5%; T = 185–215 °C) is due to the sublimation of ferrocene. The extent of this sublimation stage is a complex function of heating rate and sample characteristics. The second mass loss (13.5%, T = 248–254 °C) is mainly due to the evolution of cyclopentadiene. The third stage involves a combination of continued cyclopentadiene evolution, due to the thermal degradation of the remaining ferrocenium ions, together with chlorine evolution from thermal decomposition of the anion.

The DTA curve (Fig. 2) contains a contiguous pair of peaks. The endotherm (T = 185–215 °C) is due to the sublimation of the ferrocene. The exotherm (T = 215–254 °C) is the resultant of the processes occurring in the later stages of the decomposition described above. The final endotherm (T = 671–700 °C) is attributed to the sublimation of iron(II) chloride which is reported to occur in the range 671–674 °C [19].

Acknowledgements

We thank Professor G. M. Sheldrick for providing us with a copy of SHELXS84 prior to publication and the SERC for the provision of crystallographic and computing facilities.

References

1 J. E. Gorton, H. L. Lentzner and W. E. Watts, *Tetrahedron, 27,* 4353 (1971).
2 A. G. Landers, M. W. Lynch, S. B. Raaberg, A. L. Rheingold, J. E. Lewis, N. J. Mammano and A. Zalkin, *J. Chem. Soc., Chem. Commun.,* 931 (1976).
3 P. Carty, *Ph.D. Thesis,* University of Nottingham, 1968.
4 P. Carty and M. F. A. Dove, *J. Organomet. Chem., 28,* 125 (1971).
5 A. Haaland, *Acc. Chem. Res., 12,* 415 (1979).
6 G. E. Coats, M. L. H. Green and K. Wade, 'Organometallic Compounds, Vol. 2, The Transition Elements', Chapman and Hall, London, 1972, p. 104.
7 P. Carty and E. Metcalfe, unpublished observation.
8 W. H. Armstrong, A. Spool, G. C. Papaefthymion, R. B. Frankel and S. J. Lippard, *J. Am. Chem. Soc., 106,* 3653 (1984).
9 E. S. Raper, *J. Therm. Anal., 25,* 463 (1982).
10 M. B. Hursthouse, R. A. Jones, K. M. A. Malik and G. Wilkinson, *J. Am. Chem. Soc., 101,* 4128 (1979).
11 G. M. Sheldrick, 'SHELXS84', program for crystal structure solution, University of Gottingen, 1984.
12 G. M. Sheldrick, 'SHELX76', programs for crystal structure determination, University of Cambridge, 1976.
13 N. Walker and D. Stuart, *Acta Crystallogr., Sect. A:, 39,* 158 (1983).
14 K. S. Murray, *Coord. Chem. Rev., 12,* 1 (1974).
15 M. G. B. Drew, V. McKee and S. M. Nelson, *J. Chem. Soc., Dalton Trans.,* 80 (1978).
16 M. Rosenblum, 'Chemistry of the Iron Group Metallocenes, Part 1', Wiley, 1965, p. 34.
17 R. M. Solbrig, L. L. Duff, D. F. Shriver and I. M. Klotz, *J. Inorg. Biochem., 17,* 69 (1982).
18 K. Wieghardt, K. Pohl and W. Gebert, *Angew. Chem., Int. Ed. Engl., 22,* 727 (1983).
19 J. D. Dunitz, L. E. Orgel and A. Rich, *Acta Crystallogr., 12,* 28 (1959).
20 F. A. Cotton, *Coord. Chem. Rev., 8,* 185 (1972).
21 T. J. Kistenmacher and G. D. Stucky, *Inorg. Chem., 7,* 2150 (1968).
22 G. Constant, J. C. Davein and Y. Jeania, *J. Organomet. Chem., 44,* 353 (1972).
23 C. R. Weast (ed.), 'Handbook of Chemistry and Physics, B-98', The Chemical Rubber Co, Cleveland, Ohio, 1971–1972.
24 R. Prins, A. R. Korswagen and A. G. T. G. Kortbeek, *J. Organomet. Chem., 39,* 335 (1972).